Altered dopamine signaling and MPTP resistance in mice lacking the Parkinson's disease-associated GPR37/parkin-associated endothelin-like receptor

Daniela Marazziti*, Elisabetta Golini*, Silvia Mandillo*, Armando Magrelli*, Walter Witke†, Rafaele Matteoni*, and Glauco P. Tocchini-Valentini*‡

*Istituto di Biologia Cellulare–Consiglio Nazionale delle Ricerche and †European Molecular Biology Laboratory Mouse Biology Programme, Campus "A. Buzzati-Traverso," Via E. Ramarini 32, I-00016 Monterotondo Scalo, Rome, Italy

Communicated by Melvin I. Simon, California Institute of Technology, Pasadena, CA, May 25, 2004 (received for review January 15, 2004)

GPR37 is an orphan G protein-coupled receptor expressed in mammalian brain, and its insoluble aggregates are found in the brain samples of juvenile Parkinson's disease patients. We have produced a *Gpr37* knock-out mouse strain and identified several phenotypic features that are similar to those reported for mutants of genes encoding components of synaptic dopamine vesicles. Our results reveal an unanticipated role of GPR37 in regulating substantia nigra-striatum dopaminergic signaling. *Gpr37*$^{-/-}$ mice are viable, with normal brain development and anatomy, but they exhibit reduced striatal dopamine content, enhanced amphetamine sensitivity, and specific deficits in motor behavior paradigms sensitive to nigrostriatal dysfunction. These functional alterations are not associated with any substantial loss of substantia nigra neurons or degeneration of striatal dopaminergic afferences, the main histological marks of Parkinson's disease. The inactivation of GPR37, in fact, has protective effects on substantia nigra neurons, causing resistance to treatment with the Parkinsonian neurotoxin 1-methyl-4-phenyl-1,2,3,6-tetrahydropyridine.

The orphan G protein-coupled receptor GPR37 and related genes encode a subfamily of putative G protein-coupled receptors that are highly expressed in the mammalian central nervous system. Human and rodent GPR37 proteins are significantly homologous to the receptors for the endothelin and bombesin peptides, but their specific ligands have yet to be identified (1–3). None of the natural or synthetic molecules tested so far, including endothelins, bombesins, and related analogs, produce either specific binding or activation of intracellular signaling pathways on expression of mammalian GPR37 receptors in tissue culture cells or *Xenopus* oocytes (2, 4, 5).

GPR37 transcripts are ubiquitously expressed in human and rodent brain and particularly abundant in the corpus callosum and substantia nigra (SN). Immunohistochemical labeling has shown that, whereas most of the mouse GPR37-positive cells are 2′,3′-cyclic nucleotide 3′-phosphodiesterase-positive oligodendrocytes of fiber tracts, they also include distinct populations of neurons such as the SN dopaminergic neurons, hippocampal neurons in the CA3 region, and cerebellar Purkinje cells (6).

GPR37 has been recently shown to be a substrate of parkin and termed parkin-associated endothelin-like receptor (6). Mutations in the *parkin* gene cause autosomal recessive inherited juvenile Parkinsonism and account for the majority of cases of inherited Parkinson's disease (PD) with an early onset (<45 years of age) (7). Parkin is an E3-ubiquitin protein-ligase and a component in the proteasomal pathway (for a review, see ref. 8). When overexpressed in cell cultures, GPR37 tends to become unfolded and insoluble, and it tends to lead to unfolded protein-induced cell death, whereas the coexpression of parkin specifically ubiquitinylates GPR37 and promotes its proteosomal degradation (6). Furthermore, the insoluble form of the receptor has been found to accumulate in the frontal lobe cortex of autosomal recessive inherited juvenile Parkinsonism patients (6). These results suggest that mutant forms of parkin may be unable to correctly interact with unfolded GPR37, leading to intracellular GPR37 aggregation and to selective death of SN dopaminergic neurons, as observed in autosomal recessive inherited juvenile Parkinsonism (6).

Susceptibility to genetic and sporadic PD increases on exposure to a variety of environmental factors, including natural and synthetic toxins (9) such as the synthetic drug contaminant 1-methyl-4-phenyl-1,2,3,6-tetrahydropyridine (MPTP). In primates and mice, MPTP treatment causes the selective degeneration of SN dopaminergic neurons and is currently being used in the experimental modeling of various pathological features of Parkinson's disease (10).

To elucidate the physiological role of GPR37 in genetic and sporadic forms of PD *in vivo*, we undertook the production and phenotypic analysis of mouse strains bearing constitutive or conditional targeted mutations of the *Gpr37* gene and investigated their sensitivity to MPTP.

Materials and Methods

Targeting Vector and Generation of Mutant Mice. The *Cre* recombinase/*loxP* genetic recombination system (11) was used to produce a mutant strain carrying the *Gpr37* gene flanked by two *loxP* sites (floxed *Gpr37* allele). We inserted a single *loxP* site, derived from the pGEMloxP vector (11), into a *Pac*I site (nucleotide −2,768 upstream the translation start site) within a 9,808-bp genomic fragment (3) containing the *Gpr37* promoter, exon 1, and a 5′ portion of the intron (clone M22) (3). We inserted the *loxP*-flanked neomycin resistance (neo) expression cassette, derived from the neoflox-8 vector (11), into the *Pml*I site (nucleotide 1,099 downstream the translation start site) within the *Gpr37* intron sequence. This construct was then subcloned in the CWKO vector downstream to the thymidine kinase gene expression cassette (12). We linearized the resulting targeting vector by *Acc*65I digestion and introduced the DNA into 129P2/OlaHsd-E14.1 embryonic stem cells by electroporation, as described in ref. 11. The occurrence of correct gene targeting events was confirmed in 3 of 163 selected embryonic stem cell clones (nos. 50, 57, and 84) by Southern blot analysis with specific probes A and B (see Fig. 2*A* and data not shown). Clone no. 50 was transfected with the pCre-Pac *in vitro* expression vector (13), and Southern blot analysis was used again to confirm the *Cre* recombinase-mediated recombination, with elimination of the floxed neomycin cassette and production of the *Gpr37*^{flox} allele. *Gpr37*$^{flox/+}$ mice were obtained from germ-line mutant chimera following injection of the embryonic stem subclone no. 25 into C57BL/6J (The Jackson Laboratory) blastocysts by

NEUROSCIENCE

Abbreviations: PD, Parkinson's disease; DA, dopamine; SN, substantia nigra; MPTP, 1-methyl-4-phenyl-1,2,3,6-tetrahydropyridine; TH, tyrosine hydroxylase; CMV, cytomegalovirus.

Data deposition: The mutant alleles reported in this paper have been deposited in the Mouse Genome Database, www.informatics.jax.org [accession nos. MGI 3027992 (*Gpr37*^{tm1Gtva}) and MGI 3027995 (*Gpr37*^{tm2Gtva})].

‡To whom correspondence should be addressed. E-mail: gtocchini@ibc.cnr.it.

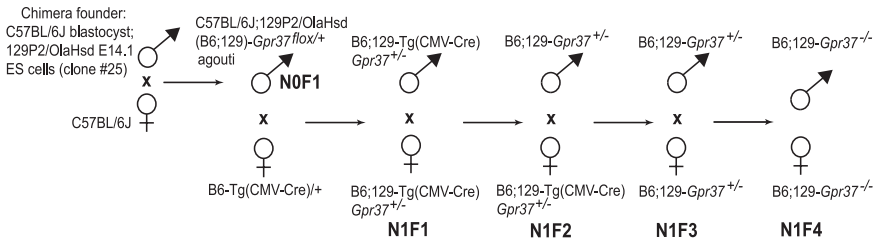

Fig. 1. Breeding of *Gpr37*$^{-/-}$ mice. The male founder was a C57BL/6J;129P2/OlaHsd (B6;129) mosaic chimera, and its mating with a B6 wild-type female produced agouti male mice, heterozygous for the *Gpr37*^{flox} allele (F1). The F1 offspring was crossed with heterozygous C57BL/6J-Tg(CMV-cre) females, carrying the *Cre* recombinase gene under the control of the human CMV minimal promoter on one of the X chromosomes. This cross generated both males and females in which the constitutive expression of the *Cre* recombinase enzyme produced the ubiquitous deletion of the *Gpr37*^{flox} allele. We thus obtained heterozygous Tg(CMV-cre) *Gpr37*$^{+/-}$ mutant mice. To eliminate the *Cre* recombinase-expressing X chromosome, we then performed three subsequent intercrosses and obtained F4 homozygous *Gpr37*$^{-/-}$ mice, with a ratio 1:4.

using standard procedures. Animals heterozygous for the disrupted *Gpr37* allele (*Gpr37*$^{-}$) were obtained by subsequent crossing (Fig. 1) of *Gpr37*$^{flox/+}$ males with C57BL/6J-Tg(CMV-cre)1Cgn (CMV-cre; Mouse Genome Database accession ID no. MGI 2176179) transgenic females that ubiquitously express the *Cre* recombinase enzyme from the embryonic two-cell stage onward, under the control of a human cytomegalovirus (CMV) minimal promoter (14). Homozygous *Gpr37*$^{-/-}$ animals, not carrying the CMV-cre transgene, were obtained according to standard breeding schemes (Fig. 1). All animals were born and bred in a specific pathogen-free facility and were subjected to experimental protocols approved by the veterinary department of the Italian Ministry of Health, according to the ethical and safety rules and guidelines for the use of animals in biomedical research provided by the relevant Italian laws and European Union's directives (n. 86/609/EC and subsequent).

PCR analysis of tail biopsy genomic DNA was undertaken by using three primers: P1-forward primer (5′-CATTGACCCAAGAATCCTACG-3′), P2-forward primer (5′-CTGTTCCATAGTTAACCTAGC-3′), and P3-reverse primer (5′-CAGGCTAGGAGCAATGGAG-3′) to amplify a 443-bp fragment specific to the wild-type allele or a 245-bp fragment specific to the disrupted *Gpr37* allele. The primers Cre-forward (5′-CGAGTGATGAGGTTCGCAAG-3′) and Cre-reverse (5′-TGAGTGAACGAACCTGGTCG-3′) were used to detect the *Cre* recombinase gene.

Northern Blot and Western Blot Analysis. Brain total RNA was extracted from 10-week-old wild-type, heterozygous and homozygous mutant mice by using TRIzol (GIBCO/BRL) and were transferred to Hybond-N^{+} nylon membranes (Amersham Pharmacia). The membranes were hybridized with specific radiolabeled probes (Fig. 2*C*), washed, and exposed under standard conditions.

Protein extracts were prepared from the striatum of wild-type and *Gpr37*$^{-/-}$ mice. The tissue samples were homogenized in lysis buffer (0.33 M sucrose/8 mM Hepes, pH 7.4/Roche complete protease inhibitors) (6), cleared by centrifugation, and the protein content of the supernatant was quantified by BCA assay (Pierce). Protein samples (30 μg) were separated by SDS/PAGE and analyzed by Western blot. Protein antigens were labeled with primary antibodies [Chemicon; mouse anti-tyrosine hydroxylase (TH), 1:1,000 dilution; rat anti-dopamine transporter, 1:10,000; rabbit anti-vesicular monoamine transporter 2, 1:1,000; sheep anti-α-synuclein, 1:2,000; rabbit anti-parkin, 1:2,000] and horseradish peroxidase-conjugated anti-mouse or anti-rabbit (Pierce), anti-rat (Amersham Pharmacia), or anti-sheep (Southern Biotechnology Associates) secondary antibodies, according to the producer's instructions. The membranes were then processed for chemiluminescence detection (SuperSignal WestDura Extended Duration Substrate, Pierce) and exposed onto radiographic film (Kodak BioMax-MS). Membranes were reprobed for α-tubulin immunolabeling as an internal control.

Measurements of Monoamines and Metabolites in Brain Tissues. Striatum and cerebellum were dissected from nine animals for each genotype (12- to 14-week-old littermates). Samples were sonicated in ice-cold 0.1 N perchloric acid/50 mg/liter sodium metabisolfite and cleared by centrifugation for 5 min at 10,000 $\times$ *g* at 4°C. The supernatants were applied to an ESA META reverse-phase HPLC column, and monoamines and metabolites were quantified with an ESA 5600 coulometric array detector (ESA-EuroService, GE-Multedo, Italy) (15).

Behavioral Tests and Data Analysis. All mutant mice and their wild-type littermates used in behavioral tests were on a 75%

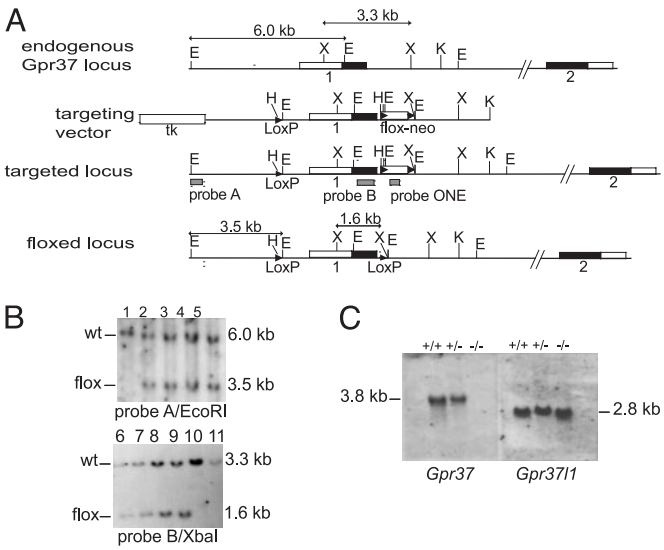

Fig. 2. Generation and characterization of *Gpr37*$^{-/-}$ mice. (*A*) Schematic representation of the *Gpr37* wild-type allele (*Top*), targeting vector, targeted allele (*Middle*), and floxed *Gpr37* locus (*Bottom*). The sites of insertion of a single *loxP* sequence (nucleotide −2,768 upstream the *Gpr37* translation start site) and the floxed neomycin resistance expression cassette (neo; nucleotide 1,099 downstream the *Gpr37* translation start site) are marked. The floxed genomic sequence that is deleted in the resulting null mutant allele comprises the entire *Gpr37* first exon encoding amino acid 1–328, the 5′-untranslated region, and a portion of the upstream promoter. Gray solid bars indicate the location of the probes used for Southern blot, along with the sizes of *Eco*RI and *Xba*I restriction fragments. The *Eco*RI (E), *Hin*dIII (H), *Kpn*I (K), and *Xba*I (X) restriction sites are shown. neo, neomycin resistance gene; tk, thymidine kinase gene. (*B*) Southern blot analysis of genomic DNA prepared from tail samples of *Gpr37*$^{flox/+}$ mice and control wild-type littermates. DNA samples were digested by *Eco*RI (lanes 1–5) and *Xba*I (lanes 6–11) and hybridized with probes A and B, which resulted in the labeling of the expected floxed bands of 3.5 kb (*Eco*RI) and 1.6 kb (*Xba*I). (*C*) Northern blot analysis of whole brain total RNA. The probes used were DNA fragments complementary to the complete cDNA sequence of the *Gpr37* or *Gpr37l1* genes (1).

C57BL/6J, 25% 129P2/OlaHsd background. All tests were carried out with male mice that were 10 weeks old at the start of the experiment. Mice were group-housed (three to five per cage) in a room with a 12-h light/dark cycle (light on at 07:00 a.m.) with ad libitum access to food and water. All behavioral studies were carried out by experimenters blind to the genotype of the animals being tested.

Open Field. Mice were tested in a rectangular open-field arena (56 × 33 cm, 28 cm high) made of white hard plastic (16). Locomotor activity was recorded with a video camera placed on the ceiling above the arena and connected to an automated video tracking system (VIDEOTRACK NT4.0, View Point, Champagne-au-Mont-d'Or, France). Consecutive 10-min intervals up to a total of 120 min of activity were recorded and analyzed. Spontaneous locomotor activity was measured as total distance traveled (in cm) during the first 30 min. The mice were then injected i.p. with either saline (0.9% wt/vol NaCl solution) or 4 mg/kg amphetamine sulfate (Sigma), and amphetamine-induced locomotor activity was recorded for the following 90 min after the injection. Due to the significant difference of spontaneous locomotor activity between genotypes, amphetamine-induced locomotor activity was expressed as a percentage of the baseline distance traveled in the last 10-min interval before the injection.

Rotarod. One week after the open-field test, mice were tested on a rotarod apparatus (Letica LE8200, Panlab, Barcelona) (17). The apparatus consisted of a rotating rod (diameter, 3 cm; hard non-slipping plastic) divided into five 5-cm lanes. On the same day of testing, mice were trained on the apparatus for at least three consecutive trials in which the rod was kept at constant speed (one trial at 0 rpm and two trials at 4 rpm). Once the trained animals were able to stay on the rod rotating at 4 rpm for 60 s, they proceeded to the test. Mice were placed individually for four consecutive trials (30-min intertrial intervals) on the rod rotating at an accelerating speed from 4 to 40 rpm in 300 s. The latency to fall off the rod and the maximal speed reached were automatically recorded.

MPTP Treatment and Measurement of Striatal MPP^+ Levels. MPTP handling and safety measures were in accordance with published guidelines (18). We used 22 mice (10- to 12-week-old male littermates of heterozygous intercross) for each genotype. Mice were housed in groups (three to five per cage) in a temperature-controlled room under a 12-h light/dark cycle with free access to food and water. On the day of the experiment, the mice received two i.p. injections of MPTP (40 mg/kg, Sigma) in saline with a 6-h interval; control mice received saline only. Seven days after the treatment, a group of mice was rapidly decapitated, and brains were removed and fixed for microtome sections. Serial coronal sections spanning the entire midbrain and the middle portion of the striatum were cut and collected for further analysis.

For the measurement of striatal MPP^+ levels, other *Gpr37*$^{-/-}$ mice and wild-type littermates were subjected to the same MPTP administration regimen and killed at 90 min after the second i.p. injection. The striatum was dissected and processed for HPLC measurement of MPP^+ as described in ref. 19 by using UV detection (wavelength, 295 nm) after separation on an ESA META 250 × 4.6 column (ESA-EuroService, GE-Multedo, Italy).

Histology, Immunohistochemistry, and Neuron Count. Age-matched brains from mutant mice and their wild-type littermates were dissected, fixed in 4% wt/vol paraformaldehyde, dehydrated, and embedded in paraffin for microtome serial sectioning (8 μm thick). Deparaffined sections were stained with cresyl-violet or processed for immunolabeling of TH (Novacastra monoclonal antibody, 1:50 dilution), glial fibrillary acidic protein (Pharmingen monoclonal antibody, 1:50), calbindin (Sigma monoclonal antibody, 1:200), 2′,3′-cyclic nucleotide 3′-phosphodiesterase (Chemicon monoclonal antibody, 1:50), myelin basic protein (Chemicon monoclonal antibody, 1:50) with a biotinylated anti-mouse secondary antibody (Vector Laboratories) and processed for diaminobenzidine-peroxidase staining (VECTASTAIN Elite ABC and DAB substrate, Vector Laboratories).

To better identify cell bodies of TH-positive neurons, the immunolabeled sections were treated with the nuclear counterstain ematoxilin (Vector Laboratories). We counted TH-positive SN pars compacta neurons in three coronal sections from two representative levels of the SN pars compacta (Bregma coordinates: −3.16; −3.52) of six to seven brains for each genotype and treatment, as described in ref. 20. The SN and the ventral tegmental area are separated at both section levels by either the medial terminal nucleus of the accessory optic tract or the medial lemniscus (20). Neurons were imaged and counted with a Leica DMLS microscope with a ×20 or ×40 objective and a CCD video camera connected to a computerized image analysis system (Leica QWin). Experimenters blind to the animal genotype and treatments selected the counting areas on scanning the entire structure of interest on the right and on the left of each section. TH-labeled neurons were scored as positive only if their cell-body image included well defined nuclear counterstaining. The same computerized image analysis system was used for the densitometric analysis of striatal TH-immunostained coronal sections at two levels (Bregma coordinates: +0.98; +1.42) of four to five brains for each genotype and treatment.

Statistical Analysis. All data were analyzed by *t* test, simple factorial ANOVA, and repeated measures ANOVA with genotype and treatment as between-subjects factors and time or trials as within-subjects factors by using STATVIEW 5.0 PowerPC software (SAS Institute, Cary, NC). *Post hoc* analysis was performed where allowed. The level of significance was set at $P < 0.05$.

Results

Generation of *Gpr37*$^{-/-}$ Mutant Mice. Using homologous recombination in 129P2/OlaHsd embryonic stem cells combined with *Cre* recombinase/*loxP* site-mediated recombination (21), we established a mouse strain carrying a mutant allele, with the *Gpr37* first exon flanked by two *loxP* sites (Mouse Genome Database symbol *Gpr37*^{tm1Gtva}, accession ID no. MGI 3027992; hereinafter floxed *Gpr37* allele or *Gpr37*^{flox}). This strain was crossed with a C57BL/6J-Tg(CMV-cre) deleter strain, which ubiquitously expresses the *Cre* recombinase enzyme already during the early phases of embryogenesis (14). In this manner, we produced a GPR37-deficient strain, carrying a *Gpr37* null mutant allele (Mouse Genome Database symbol *Gpr37*^{tm2Gtva}, accession ID no. MGI 3027995; hereinafter *Gpr37*$^{-}$; Fig. 1) in which the first exon of the *Gpr37* gene (encoding amino acids 1–328 and the 5′-untranslated region) and the upstream promoter sequences are deleted (Fig. 2 *A* and *B*).

The absence of *Gpr37* transcripts was verified by Northern blot and RT-PCR. No specific transcript was detected in the brain samples of *Gpr37*$^{-/-}$ mutant mice (Fig. 2*C* and data not shown), whereas the expression of the homologous *Gpr37l1* gene proved to be unaltered. Thus, the inactivation of *Gpr37* is not compensated for by alterations in the tissue distribution or in the levels of transcription of the related *Gpr37l1* mRNA.

Mating among heterozygous *Gpr37*$^{+/-}$ mice produced *Gpr37*$^{-/-}$ offspring with a normal Mendelian pattern of inheritance, indicating that the inactivation of the GPR37 protein does not interfere with embryonic and fetal viability. Homozygous mutant mice reached the sexual maturity at the same age as their wild-type littermates, and both *Gpr37*$^{-/-}$ females and males were fertile. A limited reduction of average body weight in comparison with wild-type littermates has been recorded ($n = 24$ for each genotype, 10- to 12-week-old males; wild-type mean body weight ± SEM = 35.8 ± 0.8 g; *Gpr37*$^{-/-}$ = 33.2 ± 0.8 g; $F_{(1,46)} = 5.26$, $P < 0.05$). Homozygous mutant mice exhibit a normal brain morphology on

NEUROSCIENCE

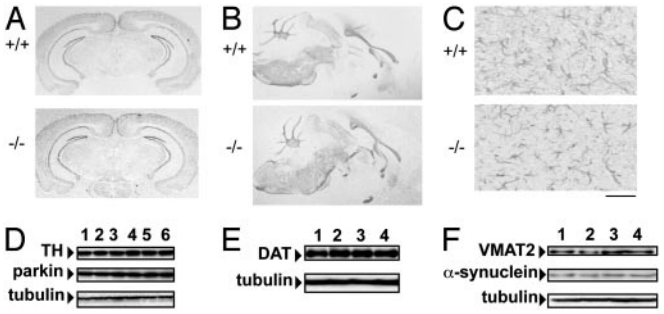

Fig. 3. *Gpr37*$^{-/-}$ mice exhibit unaltered neuroanatomy and normal Western blot staining of protein markers of dopaminergic neurons. (*A*) Nissl staining on coronal brain sections at the level of the SN of wild-type (+/+) and *Gpr37*$^{-/-}$ (−/−) mice. (*B*) 2′,3′-Cyclic nucleotide 3′-phosphodiesterase staining on sagittal brain sections of wild-type and *Gpr37*$^{-/-}$ mice. (*C*) Glial fibrillary acidic protein staining on *striatum* sections of wild-type and *Gpr37*$^{-/-}$ mice, showing similar reactive gliosis after MPTP treatment (scale bar, 100 μm). (*D*) Western blot analysis of parkin, TH, and α-tubulin in representative *striatum* samples of wild-type (lanes 1–3) or *Gpr37* null mutant mouse (lanes 4–6). (*E* and *F*) Western blot analysis of DA transporter and α-tubulin, vesicular monoamine transporter 2, α-synuclein, and α-tubulin in striatum samples of wild-type (lanes 1 and 2) and *Gpr37* null mutant mice (lanes 3 and 4).

Nissl staining, and the immunohistochemical analysis of *Gpr37*$^{-/-}$ brain sections, using antibodies specific for 2′,3′-cyclic nucleotide 3′-phosphodiesterase, myelin basic protein, and calbindin, shows that the oligodendrocytes and striatum also stain normally (Fig. 3 *A* and *B* and data not shown).

Normal Neuroanatomy of Dopamine (DA) Neurons in *Gpr37*$^{-/-}$ Mice. The most prominent neuropathological feature of autosomal recessive inherited juvenile Parkinsonism and PD is the selective loss of DA neurons in the SN (9). By means of computerized stereometric analysis (20), we quantified the number of immunolabeled TH-positive dopaminergic neurons in the SN of *Gpr37*$^{-/-}$ ($n = 6$) and wild-type 10-week-old adult males ($n = 6$). Similar numbers of TH-positive neurons were found in the SN of *Gpr37*$^{-/-}$ and the wild-type mice (see Fig. 6 *A* and *C*). We also checked for possible alterations of nigrostriatal dopaminergic afferences in *Gpr37*$^{-/-}$ animals, which may anticipate the loss of DA neurons (9). Dopaminergic projections produced normal TH cytological immunostaining (see Fig. 6*B*), and also the striatal optical density of the TH immunoreaction in *Gpr37*$^{-/-}$ mice was not significantly changed (see Fig. 6*D*) nor was any significant difference detected when comparing null mutants with wild-type littermates at 9–12 months of age (data not shown). Western blot analysis of TH also showed no significant differences between SN or striatum samples of *Gpr37*$^{-/-}$ and wild-type 10-week-old males (Fig. 3*D*). Similar results were obtained for parkin (Fig. 3*D*), in agreement with the hypothesis that parkin expression is mainly up-regulated on overexpression of GPR37 (6). Western blot analysis also did not reveal significant variations (Fig. 3 *E* and *F*) of the level of α-synuclein, another parkin substrate, and of components of the nigro-striatal dopaminergic pathway, including the plasma membrane DA transporter and the vesicular monoamine transporter 2.

Reduction of Striatal DA Content in Mutant Mice. To see whether the absence of GPR37 was associated with alterations in the striatal or cerebellar content of DA or of other neurotransmitters and their metabolites, we carried out a quantitative coulometric analysis by HPLC. The average DA content was reduced by 10.6% in the striatum of homozygous mutant mice in comparison to wild-type littermates (12- to 13-week-old males, *t* test, $P < 0.05$; Fig. 4*A*).

No significant differences were detected in the striatum content of the DA catabolites dihydrophenylacetic acid, homovanillic acid,

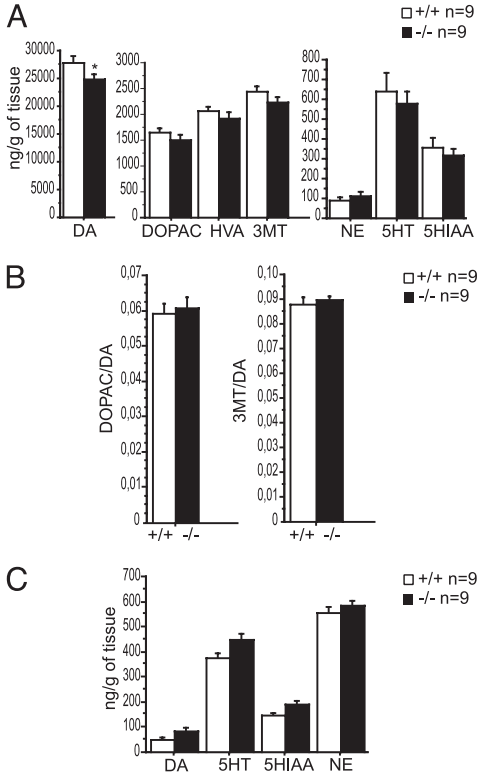

Fig. 4. Quantification by HPLC of striatal dopamine metabolite ratios and of cerebellar monoamines and metabolite levels in *Gpr37*$^{-/-}$ and wild-type littermate mice. (*A*) Quantification of monoamines and metabolite levels in *Gpr37*$^{-/-}$ and wild-type littermate mice. DA, norepinephrine (NE), and serotonin (5-HT) as well as their metabolites, dihydrophenylacetic acid (DOPAC), homovanillic acid (HVA), 3-methoxytiramine hydrochloride (3-MT), and 5-hydroxyndolacetic acid (5-HIAA) were measured in perchloric acid extracts prepared from striatum of wild-type ($n = 9$) and *Gpr37*$^{-/-}$ ($n = 9$) mice by using HPLC with coulometric detection. The average DA content in the *striatum* of null mutant animals was significantly reduced (−10.6%; *, $P < 0.05$, *t* test). Other monoamine and metabolite levels did not vary significantly. Results are presented as mean ± SEM. (*B*) dihydrophenylacetic acid:DA and 3-methoxytiramine hydrochloride:DA content ratios were measured in perchloric acid extracts prepared from striatum samples of wild-type (+/+; $n = 9$) and *Gpr37*$^{-/-}$ (−/−; $n = 9$) mice. (*C*) DA, norepinephrine, serotonin, and 5-hydroxyndolacetic acid were measured in perchloric acid extracts prepared from cerebellum samples of wild-type ($n = 9$) and *Gpr37*$^{-/-}$ ($n = 9$) mice. Results are presented as mean values ± SEM.

and 3-methoxytiramine hydrochloride (Fig. 4*A*), or in the DA catabolites dihydrophenylacetic acid:DA and 3-methoxytiramine hydrochloride:DA ratio (Fig. 4*B*), which are standard parameters of the relative rate of intraneuronal and extracellular DA catabolism, respectively (22), nor was there any significant difference in the cerebellar content of DA and DA catabolites, or in the content of norepinephrine, serotonin, and of the serotonin catabolite 5-hydroxyndolacetic acid in either striatum (Fig. 4*A*) or cerebellum samples (Fig. 4*C*). These data are consistent with the hypothesis that the reduction of DA content in the striatum of *Gpr37*$^{-/-}$ mice may be primarily due to decreased DA synthesis or vesicular storage in presynaptic SN neurons. Significant alterations in the level of catabolites produced by synaptic DA release or intracellular DA turnover were in fact not detected.

Alteration of Spontaneous and Amphetamine-Induced Locomotor Activity in Mutant Mice. We also analyzed *Gpr37*$^{-/-}$ mice for possible alterations in behavioral paradigms sensitive to dysfunction of the nigrostriatal dopaminergic pathway. Locomotor activity was tested by using the open-field and rotarod task assays. These tests

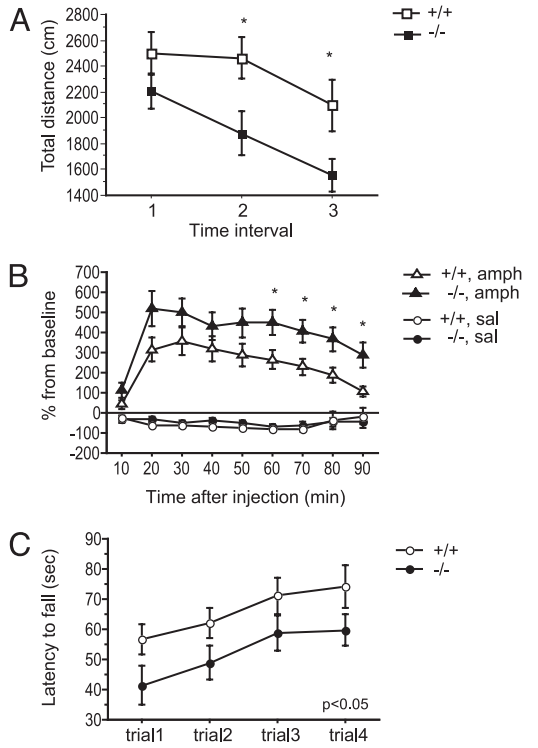

Fig. 5. *Gpr37* null mutant mice differ in spontaneous and amphetamine-induced locomotor activity and motor coordination. (*A*) Spontaneous locomotor activity measured for 30 min in a rectangular open-field arena. Open (wild-type: +/+) and solid (null mutant: −/−) squares ($n = 24$ per genotype) represent mean ± SEM total distance traveled (cm) in each 10-min interval. *, $P < 0.05$, wild-type vs. *Gpr37*$^{-/-}$ animals (*t* test). (*B*) Amphetamine-induced locomotor activity in wild-type and *Gpr37* null mutant mice. *Gpr37*$^{-/-}$ mice showed a higher amphetamine-induced increase of locomotor activity in comparison with wild-type littermates. Open (+/+) and solid (−/−) circles (saline) and triangles (amphetamine) represent mean ± SEM distance (cm) traveled expressed as percentage of baseline locomotor activity measured before the injection (last 10-min interval of spontaneous locomotion; Fig. 2*B*). *, $P < 0.05$, wild-type vs. *Gpr37*$^{-/-}$ animals (*t* test). (*C*) *Gpr37* null mice show impairment in motor coordination as measured with the rotarod test. Open (+/+) and solid (−/−) circles ($n = 20$ per genotype) represent mean ± SEM latency to fall off a rotating rod accelerating from 4 to 40 rpm in 300 s over four consecutive trials.

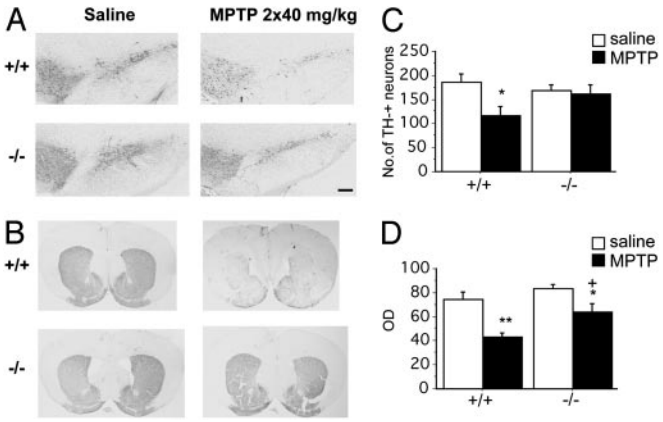

Fig. 6. *Gpr37* null mutant mice display normal neuroanatomy of SN dopaminergic neurons and are resistant to MPTP-induced neurodegeneration. *Gpr37*$^{-/-}$ mice and wild-type littermates were treated with two i.p. injections (saline or 40 mg/kg MPTP in saline) with a 6-h interval. Brains were removed 7 days after the treatment. (*A* and *B*) TH immunostaining of SN pars compacta (SNc) or striatum in wild-type and *Gpr37*$^{-/-}$ mice treated with saline or MPTP. Nissl staining confirmed the pattern of TH immunostaining (data not shown). (*C*) Number of SN pars compacta TH immunoreactive dopaminergic neurons (*, $P < 0.05$ vs. saline-treated wild-type animals; saline-treated wild-type, $n = 6$; saline-treated *Gpr37*$^{-/-}$, $n = 6$; MPTP-treated wild-type, $n = 6$; MPTP-treated *Gpr37*$^{-/-}$, $n = 7$). (*D*) Optical density (OD) quantification of the intensity of immunostaining of striatal TH-positive SN projections (**, $P < 0.005$ vs. saline-treated wild-type; *, $P < 0.05$ vs. saline-treated *Gpr37*$^{-/-}$; +$P < 0.05$ vs. MPTP-treated wild-type; saline-treated wild-type, $n = 4$; saline-treated *Gpr37*$^{-/-}$, $n = 4$; MPTP-treated wild-type, $n = 5$; MPTP-treated *Gpr37*$^{-/-}$, $n = 5$). The results are presented as mean ± SEM. (Scale bar, 200 μm.)

are used to measure rodent locomotion and motor coordination in a standardized manner, so as to evaluate brain functions that are mainly affected by functional alterations of the dopaminergic systems (16, 17).

The spontaneous locomotor activity of the mice (10- to 12-week-old males) was measured for 30 min in an open-field arena. Homozygous mutant mice showed reduced locomotor activity in comparison with their wild-type littermates, and this genotype effect [$F_{(1, 46)} = 4.99$, $P < 0.05$; Fig. 5*A*] was more pronounced in the last phase of the test.

The increase of locomotor activity induced by D-amphetamine in the same groups of mice was subsequently measured for 90 min (Fig. 5*B*). All amphetamine-treated mice (4 mg/kg i.p. injection) displayed increased locomotor activity in comparison with saline-treated mice [RM ANOVA, treatment factor: $F_{(1, 44)} = 98.20$, $P < 0.0001$], although *Gpr37*$^{-/-}$ mice proved to be more sensitive to the amphetamine treatment [RM ANOVA, genotype factor: $F_{(1, 44)} = 5.15$, $P < 0.05$; genotype × treatment factor, $F_{(1, 44)} = 4.06$, $P = 0.05$]. Again, the genotype effect showed a time-dependent increase.

One week after the open-field test, the same group of mice was subjected to four consecutive trials on a rotarod apparatus (4–40 rpm acceleration in 300 s) in which homozygous mutant mice exhibited latencies to fall from the rotating rod that were significantly shorter than those of the wild-type ones [$F_{(1, 38)} = 5.09$, $P < 0.05$; Fig. 5*C*]. Statistical analyses revealed no significant correlation between the reduction of body weight of *Gpr37*$^{-/-}$ mice and their open-field or rotarod test scores (data not shown).

Gpr37-Null Mutant Mice Are Resistant to MPTP. The sensitivity to the Parkinsonian neurotoxin MPTP was studied in 10- to 12-week-old *Gpr37*$^{-/-}$ mice ($n = 22$) and wild-type littermates ($n = 22$) by subjecting them to two i.p. injections (6-h interval) of either a pure saline solution or of 40 mg/kg MPTP in saline solution. Two days postinjection, survival rates were noted. Among the MPTP-treated animals, 6 of 13 wild-type and 2 of 13 *Gpr37*$^{-/-}$ mice were found dead. After 7 days, the survived animals were killed, and brains were removed and processed for immunohistochemical labeling of TH and glial fibrillary acidic protein, followed by stereometric counting of TH-positive SN neurons and optical density measurement of striatal terminals. *Gpr37*$^{-/-}$ mice were distinctly those most resistant to MPTP treatment, manifesting a reduced MPTP-induced degeneration of TH-positive SN neurons (Fig. 6 *A* and *C*) and striatal nerve terminals (Fig. 6 *B* and *D*), in comparison with wild-type animals, along with a much higher survival rate (84% as compared with 53%).

The level of the active MPTP metabolite 1-methyl-4-phenylpyridinium (MPP^+) in striatal samples was also measured by HPLC, and we detected no significant genotype difference. MPP^+ levels 90 min after the final i.p. injection of MPTP were as follows: wild type = 15.4 ± 0.4, *Gpr37*$^{-/-}$ = 16.3 ± 0.5 μg/g striatal tissue ($n = 3$ for each genotype). Glial fibrillary acidic protein immunolabeling also showed unaltered MPTP-induced reactive gliosis in *Gpr37*$^{-/-}$ mice (Fig. 3*C*). Thus, the *Gpr37*$^{-/-}$ resistance to MPTP treatment is not due to alteration of MPTP toxicokinetics and of microglia activation.

Discussion

The GPR37 orphan receptor is a substrate of parkin that accumulates in the brain of autosomal recessive inherited juvenile Parkinsonism patients, and its experimental overexpression in neuronal cell cultures and in neurons of transgenic *Drosophila* strains leads to selective neuronal death (6, 23). The data reported in this paper show that loss-of-function mutations of the mouse *Gpr37* gene cause a reduction in striatal DA content, specific locomotor deficits with enhanced sensitivity to amphetamine, and resistance to treatment with the Parkinsonian neurotoxin MPTP; these phenotypic characteristics, moreover, may be associated with alterations of the nigrostriatal dopaminergic signaling pathway (10). On the other hand, no loss of DA neurons in the SN or degeneration of dopaminergic striatal afferences was observed in the $Gpr37^{-/-}$ mice. These results suggest that the functional alterations underlying the $Gpr37^{-/-}$ motor deficits differ from those involved in the movement disorders characteristic of PD, which instead result primarily from degeneration and substantial loss of SN dopaminergic neurons (9). In fact, contrary to what has been observed on its experimental overexpression (6, 23), the genetic inactivation of GPR37 has protective effects on SN dopaminergic neurons, inducing resistance of $Gpr37^{-/-}$ mice to MPTP treatment. Although its original biochemical mechanisms have yet to be elucidated, the protection from MPTP toxicity is similar to that observed in several strains carrying null mutations of genes expressed in the SN (24–29). The protective effect of GPR37 inactivation is more marked on the TH-positive neuronal cell bodies in the SN than on dopaminergic synaptic terminals in the striatum (Fig. 6 *C* and *D*). Interestingly, similar results have been reported for mice carrying null mutations of other genes that encode proteins associated with the MPTP-induced degeneration of dopaminergic neurons, such as microglial NOS_2, which is responsible for increased synthesis of nitric oxide, an oxidant molecule crucially involved in MPTP neurotoxicity (27), or TNFRSF6/FAS, which has recently been shown to regulate inflammatory neurodegeneration in an MPTP model of PD (29).

We report five phenotypic traits of $Gpr37^{-/-}$ mice (reduction of body weight, decrease of striatum DA content, increased sensitivity to amphetamine treatment, specific locomotor and motor coordination deficits in open-field and rotarod tests) that are qualitatively similar to some of the features identified in heterozygous knock-out mutant strains of the *Vmat2* gene, which encodes the synaptic vesicle membrane DA transporter (28, 30, 31). Taken together, our findings suggest that GPR37, too, may be implicated in the regulation of the assembly or trafficking of synaptic DA vesicles. The reduction of striatal DA content and the specific locomotor deficits in open-field and rotarod tests of $Gpr37^{-/-}$ mice may therefore be due to underlying alterations in the releasable pool of striatal presynaptic DA vesicles (26). Comparable results have been described for certain viable heterozygous $Vmat2^{+/-}$ mutants, which exhibit increased sensitivity to amphetamine treatment (30, 31). The latter is also a remarkable feature of the $Gpr37^{-/-}$ strain; moreover, the effects of the $Gpr37^{-/-}$ (Fig. 5 *A* and *B*) and $Vmat2^{+/-}$ genotypes (30, 31) on both spontaneous locomotion and amphetamine sensitivity show a tendency to increase over time. One might speculate that the slight reduction ($\approx$10%) of the presynaptic DA vesicular pool in untreated $Gpr37^{-/-}$ mice could initially induce a limited decrease of spontaneous locomotion, whereas at later times the cumulative effects on vesicle metabolism would result in a more robust locomotor inhibition. The depletion of DA in the vesicle pool, furthermore, may produce an increase of its cytoplasmic concentration, with an augmented unregulated efflux via exchange diffusion by DA transporter, on administration of amphetamine (28, 30, 31). These conditions might in turn lead to sustained stimulation of TH activity and DA synthesis, which would explain the prolonged and increasing effects of amphetamine on the locomotor activity of $Gpr37^{-/-}$ mice (Fig. 5*B*).

The data that we have collected demonstrate the unexpected involvement of GPR37 in the complex network of components that regulate the metabolism of SN neurons and the functionality of the nigrostriatal dopaminergic pathway. It is now possible to cross the $Gpr37^{-}$ and $Gpr37^{flox}$ mutants that become available with other mutant strains (24–33) and to produce and phenotypically characterize primary cell cultures and *in vivo* animal models with multiple, constitutive or conditional targeted mutations of the components of dopaminergic signaling pathway. Furthermore, the $Gpr37^{-/-}$ mutant strain will be instrumental for carrying out *in vivo* studies on the mechanisms of action of MPTP and other neurotoxins and for the pathological and pharmacological modeling of drug addiction and behavioral disorders.

We thank K. Rajewsky and R. Kühn for the gift of the pGEMloxP and neoflox-8 vectors and the CMV-cre mouse transgenic strain, J. K. Barrett for blastocyst injection, E. Pearl for assistance with histological techniques, G. Di Franco and G. D'Erasmo for excellent technical assistance, and A. Ferrara for secretarial work. This work was supported by Italian Ministry of Research projects (Consiglio Nazionale delle Ricerche Biomolecole per la Salute Umana-L.95/95-5%, Genetica Molecolare and Genomica Funzionale; FIRB Progetti Negoziali 2001 and 2003) and by the EUMORPHIA (QLG2-CT-2002-00930) and MUGEN European Networks of Excellence.

1. Marazziti, D., Golini, E., Magrelli, A., Matteoni, R. & Tocchini-Valentini, G. P. (2001) *Curr. Genomics* **2,** 253–260.
2. Marazziti, D., Golini, E., Gallo, A., Lombardi, M. S., Matteoni, R. & Tocchini-Valentini, G. P. (1997) *Genomics* **45,** 68–77.
3. Marazziti, D., Gallo, A., Golini, E., Matteoni, R. & Tocchini-Valentini, G. P. (1998) *Genomics* **53,** 315–324.
4. Zeng, Z., Su, K., Kyaw, H. & Li, Y. (1997) *Biochem. Biophys. Res. Commun.* **233,** 559–567.
5. Leng, N., Gu, G., Simerly, R. B. & Spindel, E. R. (1999) *Brain Res. Mol. Brain Res.* **69,** 73–83.
6. Imai, Y., Soda, M, Inoue, H., Hattori, N., Mizuno, Y. & Takahashi, R. (2001) *Cell* **105,** 891–902.
7. Kitada, T., Asakawa, S., Hattori, N., Matsumine, H., Yamamura, Y., Minoshima, S., Yokochi M., Mizuno, Y. & Shimizu, N. (1998) *Nature* **392,** 605–608.
8. Feany, M. B. & Pallanck, L. J. (2003) *Neuron* **38,** 13–16.
9. Langston, J. W., Ballard, P., Tetrud, J. W. & Irwin, I. (1983) *Science* **219,** 979–980.
10. Dauer, W. & Przedborski, S. (2003) *Neuron* **39,** 889–909.
11. Torres, R. T. & Kuhn, R. (1997) in *Laboratory Protocols for Conditional Gene Targeting* (Oxford Univ. Press, London).
12. Westphal, C. H. & Leder, P. (1997) *Curr. Biol.* **7,** 530–533.
13. Taniguchi, M., Sanbo, M., Watanabe, S., Naruse, I., Mishina, M. & Yagi, T. (1998) *Nucleic Acids Res.* **26,** 679–680.
14. Schwenk, F., Baron, U. & Rajewsky, K. (1995) *Nucleic Acids Res.* **23,** 5080–5081.
15. Seegal, R. F., Brosch, K. O. & Bush, B. (1986) *J. Chromatogr.* **377,** 131–144.
16. Fernagut, P. O., Chalon, S., Diguet, E., Guilloteau, D., Tison, F. & Jaber, M. (2003) *Neuroscience* **116,** 1123–1230.
17. Rozas, G., Lopez-Martin, E., Guerra, M. J. & Labandeira-Garcia, J. L. (1998) *J. Neurosci. Methods* **83,** 165–175.
18. Przedborski, S., Jackson-Lewis, V., Naini, A. B., Jakowec, M., Petzinger, G., Miller, R. & Akram, M. (2001) *J. Neurochem.* **76,** 1265–1274.
19. Battaglia, G., Busceti, C. L., Molinaro, G., Biagioni, F., Storto, M., Fornai, F., Nicoletti, F. & Bruno, V. (2004) *J. Neurosci.* **24,** 828–835.
20. Kuhn, K., Wellen, J., Link, N., Maskri, L., Lubbert, H. & Stichel, C. C. (2003) *Eur. J. Neurosci.* **17,** 1–12.
21. Lewandoski, M. (2001) *Nat. Rev. Genet.* **2,** 743–755.
22. Horger, B. A., Nishimura, M. C., Armanini, M. P., Wang, L. C., Poulsen, K. T., Rosenblad, C., Kirik, D., Moffat, B., Simmons, L., Johnson, E., *et al.* (1998) *J. Neurosci.* **18,** 4929–4937.
23. Yang, Y., Nishimura, I., Imai, Y., Takahashi, R. & Lu, B. (2003) *Neuron* **37,** 911–924.
24. Dauer, W., Kholodilov, N., Vila, M., Trillat, A. C., Goodchild, R., Larsen, K. E., Staal, R., Tieu, K., Schmitz, Y., Yuan, C. A., *et al.* (2002) *Proc. Natl. Acad. Sci. USA* **99,** 14524–14529.
25. Schluter, O. M., Fornai, F., Alessandri, M. G., Takamori, S., Geppert, M., Jahn, R. & Sudhof, T. C. (2003) *Neuroscience* **118,** 985–1002.
26. Abeliovich, A., Schmitz, Y., Farinas, I., Choi-Lundberg, D., Ho, W. H., Castillo, P. E., Shinsky, N., Verdugo, J. M., Armanini, M., Ryan, A., *et al.* (2000) *Neuron* **25,** 239–252.
27. Liberatore, G. T., Jackson-Lewis, V., Vukosavic, S., Mandir, A. S., Vila, M., McAuliffe, W. G., Dawson, V. L., Dawson, T. M. & Przedborski, S. (1999) *Nat. Med.* **5,** 1403–1409.
28. Takahashi, N., Miner, L. L., Sora, I., Ujike, H., Revay, R. S., Kostic, V., Jackson-Lewis, V., Przedborski, S. & Uhl, G. R. (1997) *Proc. Natl. Acad. Sci. USA* **94,** 9938–9943.
29. Hayley, S., Crocker, S. J., Smith, P. D., Shree, T., Jackson-Lewis, V., Przedborski, S. Mount, M., Slack, R., Anisman, H. & Park, D. S. (2004) *J. Neurosci.* **24,** 2045–2053.
30. Fon, E. A., Pothos, E. N., Sun, B. C., Killeen, N., Sulzer, D. & Edwards, R. H. (1997) *Neuron* **19,** 1271–1283.
31. Wang, Y. M., Gainetdinov, R. R., Fumagalli, F., Xu, F., Jones, S. R., Bock, C. B., Miller, G. W., Wightman, R. M. & Caron, M. G. (1997) *Neuron* **19,** 1285–1296.
32. Itier, J-M., Ibanez, P., Mena, M. A., Abbas, N., Cohen-Salmon, C., Bohme, G. A., Laville, M., Pratt, J., Corti, O., Pradier, L., *et al.* (2003) *Hum. Mol. Genet.* **12,** 2277–2291.
33. Goldberg, M. S., Fleming, S. M., Palacino, J. J., Cepeda, C., Lam, H. A., Bhatnagar, A., Meloni, E. G., Wu, N., Ackerson, L. C., Klapstein, G. J., *et al.* (2003) *J. Biol. Chem.* **278,** 43628–43635.